ADVANCED FUNCTIONAL MATERIALS
www.afm-journal.de

Photoinduced Anisotropic Supramolecular Assembly and Enhanced Charge Transport of Poly(3-hexylthiophene) Thin Films

*Mincheol Chang, Jiho Lee, Nabil Kleinhenz, Boyi Fu, and Elsa Reichmanis**

The self-organization of organic polymer semiconductors into ordered supramolecular assemblies commensurate with efficient charge transport is achieved by tuning a range of process parameters (e.g., film deposition method (spin vs drop cast), solvent boiling point (low vs high boiling point), polymer-dielectric interface treatment, and post-deposition processing (solvent vapor or thermal annealing)). However, these strategies present limitations for large-scale high-throughput processing due to associated pre- and/or post semiconductor deposition steps. Here, photoinduced anisotropic supramolecular assembly of P3HT chains in solution is demonstrated. UV irradiation provides for enhanced intramolecular ordering of solubilized polymer chains, and thereby effects formation of anisotropic supramolecular polymer assemblies via favorable π–π stacking (intermolecular interaction). Molecular ordering is thus dramatically enhanced with concomitant, enhanced charge transport characteristics of corresponding films. Additional pre- and/or post treatments are avoided.

1. Introduction

Conjugated polymer semiconductors have garnered interest for application as opto-electronic device components, because they may provide for low-cost, large-area electronic device fabrication arising from their low-temperature, solution-based processability.[1] These polymers exhibit anisotropic optical and electrical properties owing to one-dimensional *p*-orbital overlap along the polymer backbone. Thus, their interesting properties can be realized in opto-electronic devices when the polymer chains are well-ordered via π–π interactions.[2] However, polymer semiconductors often suffer from relatively low charge carrier transport characteristics owing to a low degree of π-stacking between polymer chains in solidified thin-films; semiconducting polymer films prepared via solution-processing are typically composed of many small crystalline regions embedded within a largely disordered matrix which may be unfavorable for efficient charge hopping between transport sites.[3] Regioregular poly (3-hexylthiophene) (P3HT) is a readily available polymer semiconductor that can serve as a model system to investigate the critical role played by polymer thin-film morphology. P3HT self-organizes into a microcrystalline structure,[4] exhibits acceptable hole transport properties,[5] and exhibits good solubility in various organic solvents.[3c] The self-organization of the polymer into ordered supramolecular assemblies commensurate with efficient charge transport has been achieved by tuning a range of process parameters (e.g., film deposition method (spin vs drop cast),[6] solvent boiling point (low vs high boiling point),[7] polymer-dielectric interface treatment,[8] and post-deposition processing (solvent vapor or thermal annealing)[9] in combination with approaches such as improved molecular design[4] and increased polymer molecular weight (MW).[10] However, these strategies present limitations for large-scale high-throughput processing due to associated pre- and/or post semiconductor deposition steps. To eliminate the need for ancillary, potentially cumbersome and costly thin-film deposition processes, several approaches including solvent solubility tuning,[11] solution aging,[12] and ultrasonic irradiation[13] have been explored to induce well-ordered nanofibrillar aggregates in solution, prior to film deposition. Self-assembled P3HT nanofibers exhibit dramatically improved crystallinity and macroscopic charge transport characteristics compared to a comparatively more amorphous P3HT film, owing to enhanced π–π interactions between conjugated chains.[13a] The anisotropic growth of crystalline-like P3HT aggregates is ascribed to strong π–π interactions in direction of the fiber axis, along which charge transport readily occurs.[13b,14] Accordingly, longer P3HT nanofibers may be expected to exhibit more effective charge transport in macroscopic polymer thin-films, owing to long-range ordered crystalline regimes. Among the effective strategies, ultrasonic irradiation leads to the formation of ordered nanofibrillar aggregates of P3HT in solution, where the concentration of aggregates can be controlled by sonication

M. Chang, J. Lee, B. Fu, Prof. E. Reichmanis
School of Chemical and Biomolecular Engineering
Georgia Institute of Technology
Atlanta, GA 30332, USA
E-mail: ereichmanis@chbe.gatech.edu
Prof. E. Reichmanis
School of Materials Science and Engineering
Georgia Institute of Technology
Atlanta, GA 30332, USA
N. Kleinhenz, Prof. E. Reichmanis
School of Chemistry and Biochemistry
Georgia Institute of Technology
Atlanta, GA 30332, USA

DOI: 10.1002/adfm.201400523

time.[13a] Alternative approaches require steps such as the addition of small quantities of poor solvent to the majority solution, and/or aging the solutions to obtain well-ordered nanofibrillar structures.[11a,12] The apparent solution based aggregates appear to persist through the deposition process, and nanofibrillar features are perceptible in what are believed to be crystalline regimes in the corresponding solid state films.[13a] Further, the resultant films exhibit a one to two order of magnitude enhancement in the corresponding field-effect mobilities. Thus, additional pre- or post-treatments to enhance crystallinity and concomitantly, charge transport characteristics, are not essential.[13a] However, P3HT nanofibers formed by ultrasonic irradiation appear to be short. While brief sonication times promote P3HT nanofibrillar aggregate formation, the treatment limits continuous fiber growth (<400 nm) presumably due to strong agitation, leading to an increase in the number of grain boundaries in resultant thin-films and thus, continued enhancement in charge carrier transport is restricted.[6,13a] Further, the ultrasonic irradiation process requires immersion of the solution into a water bath and is sensitive to a number of experimental parameters, many of which may be difficult to control, thus complicating the experimental results and presenting its own set of scale-up challenges. Herein, we demonstrate for the first time, a facile, scalable strategy to enhance anisotropic supramolecular ordering of P3HT chains in solution using low intensity, limited duration ultraviolet (UV) irradiation. UV treatment of the conjugated polymer solution enhances crystallinity and concomitantly, charge transport characteristics of resultant thin-films. The approach represents a benign alternative for large-scale fabrication and high-throughput processing of polymer-based devices for a range of applications due to the ease with which the polymer solutions could be exposed uniformly to UV light. The apparently crystalline nanofibrillar aggregates formed by UV irradiation are greater than 1 µm in length, which is likely the origin of the improvement in charge carrier mobility for films deposited from the irradiated solutions versus those prepared via ultrasonication.

2. Results and Discussion

Bottom contact organic field-effect transistors (OFETs) (**Figure 1**a) were fabricated by spin-coating the respective P3HT solutions onto device substrates (transistor channel width = 2000 µm and length = 50 µm) using P3HT/chloroform ($CHCl_3$) (5 mg mL^{-1}) solutions irradiated by a UV lamp (Entela UVGL-15, 5 mW cm^{-2}, 254 nm) for designated times. Figure 1b depicts the observed dramatic increase in the mobility of these

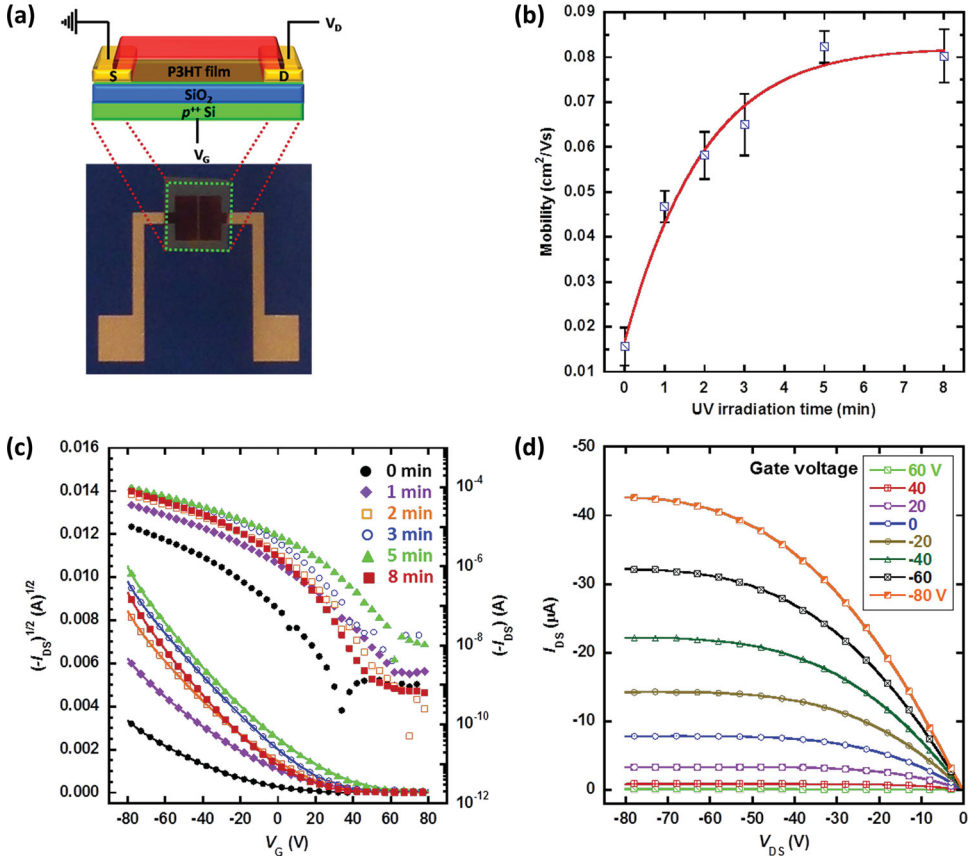

Figure 1. a) Schematic structure and photoimage of OFET device. b) Average field-effect mobilities of P3HT films spin coated from P3HT/$CHCl_3$ solutions irradiated by UV for designated times. Mobilities were calculated in the saturation regime of operation with V_{DS} = –80 V. c) Transfer characteristics of P3HT OFETs fabricated from UV irradiated polymer solutions. d) Typical output characteristics obtained from a P3HT OFET prepared via spin-coating from P3HT/$CHCl_3$ solution UV irradiated for 8 min. All measurements were performed in a nitrogen glovebox.

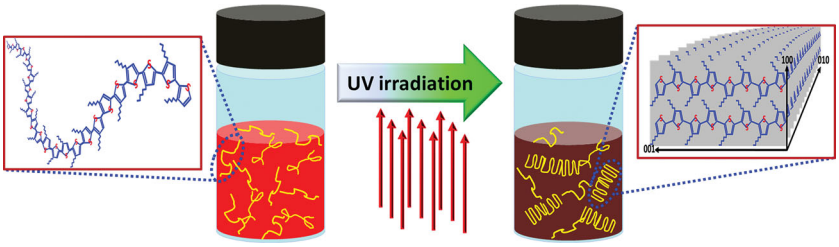

Figure 2. a) Suggested mechanism for the UV irradiation induced anisotropic molecular ordering of P3HT chains.

P3HT films as a function of UV irradiation time. The observed increase is greater than that obtained with films prepared via ultrasonication (see Figure S1, Supporting Information); while ultrasonication processing of the P3HT sample used here afforded approximately a 4.6-fold (from $1.6 \pm 0.42 \times 10^{-2}$ to $7.3 \pm 0.55 \times 10^{-2}$ cm^2 V^{-1} s^{-1}) increase in macroscopic hole mobility, UV irradiation provided for more than a 5.1-fold enhancement (up to $8.2 \pm 0.35 \times 10^{-2}$ cm^2 V^{-1} s^{-1}). Moreover, the mobility of poly(3-butylthiophene) (P3BT) films was enhanced almost 10.7-fold (from $1.3 \pm 0.11 \times 10^{-3}$ to $13.9 \pm 1.00 \times 10^{-3}$ cm^2 V^{-1} s^{-1}) via UV irradiation, while ultrasonication led to an increase of only approximately 3.5-fold (up to $4.5 \pm 0.41 \times 10^{-3}$ cm^2 V^{-1} s^{-1}) (see Figure S2, Supporting Information). Saturation of mobility is discerned upon UV irradiation for times in the range of 5 to 8 min. The observation of the saturation is reminiscent of the percolation type transport mechanism proposed for P3HT thin-films prepared from ultrasonicated solutions.[13a] Figures 1c and d depict transfer and characteristic output curves, respectively, which are typical of p-channel OFET operation in the accumulation mode. The high turn-on voltages (V_{ON}) obtained in Figure 1c are attributed to the effects of residual doping, acceptor like traps at the P3HT-oxide interface, and/or charge trapping at grain boundaries/interfaces.[6,15]

Figure 2 presents a schematic illustration of a suggested mechanism for the observed UV induced anisotropic supramolecular ordering of P3HT chains in solution. Photoexcitation is known to effect charge injection into conjugated polymers such as polythienylenes, resulting in local structural distortion and the formation of self-localized polarons or bipolarons with associated electronic states in the energy gap.[16] In the ground state, the conjugated segments of polythiophenes are largely aromatic in character, while the excited states are stabilized as self-localized regions of the chain within which bond alternation is shifted to a more stable conformation (i.e., quinoid character), which exhibits an intrinsically higher degree of coplanarity and conceivably enhanced neighboring π–π interactions.[16,17] Based on quantum chemical calculations, the self-localized states are extended over 4 to 5 rings.[16a,18] In a typical experiment, the P3HT solution is gently stirred in a borosilicate glass vial which is more than 90% transmissive at 254 nm, and it is then irradiated. Upon UV irradiation, the conjugated polymer (in solution) becomes photoexcited; while in the ground state π-electrons are localized through π-orbital overlap within thiophene rings, they are more effectively delocalized along the polymer backbone through enhanced π-orbital overlap between individual thiophene rings in the excited state.[16,19] The increased π-orbital overlap may lead to planarization of the polymer backbone, and effect a change in polymer solubility.[16,17,19,20] A more rigid backbone is expected to decrease solubility and thereby favor P3HT π–π interchain interactions, which over time afford extended supramolecular assemblies of the conjugated polymer.[17a,20]

It is generally known that UV irradiation, coupled with exposure to oxygen and water, can lead to significant polymer degradation, diminishing polymer properties.[21] No discernible P3HT degradation was observed here (see Supporting Information Table S1,S2 and Figure S3–S5). The effect of UV irradiation was found to be thermally reversible as shown in Figure S6, Supporting Information; the solution absorption spectra and colors changed through UV irradiation were restored to those of pristine P3HT solutions via mild heating. It is believed that the exposure dose (5 mW cm^{-2} for ≈8 min under air) used for even the highest dose is relatively mild compared to that required for polymer degradation (reported as 130 mW cm^{-2} for ≈1000 min under oxygen atmosphere).[22]

Figure 3a,b depict the electronic absorption spectra obtained from P3HT/$CHCl_3$ solutions irradiated by UV for times ranging from 0 to 8 min, and spectra acquired from the corresponding semiconducting thin-films, respectively. The solution changed from bright orange to dark brown with increased UV irradiation time (inset in Figure 3a), indicative of an increase in P3HT nanoaggregate concentration.[13a] The solution based absorption spectra exhibit low energy features at ≈570 and 620 nm, suggestive of vibronic bands associated with the (0–1) and (0–0) transitions respectively, which increase with increased UV irradiation time. The emergence of these features is believed to be associated with an increase in ordered aggregates formed via π–π stacking between polymer chains in solution (Figure 3a).[13a] In the present case, the vibronic features are suggested to result directly from UV induced anisotropic extension of P3HT chains in solution, that is, photoinduced polymer chain planarization (intramolecular ordering) followed by ordered aggregate formation (intermolecular ordering).

Consistent with previous reports,[6,13a] the solution based nanoaggregates appear to survive a spin-coating process, and in turn provide for increased molecular order in the solid thin-films as shown in Figure 3b; resultant films transform from pale red to dark purple with increased irradiation time (inset in Figure 3b). Further, as the irradiation time of the solutions increases, the low energy absorption bands at ≈555 and 605 nm appear to increase in intensity in resultant polymer films, supporting the presumption that ordered P3HT nanoaggregates in solution survive the thin-film deposition process. While in the solid films, the lower energy bands exhibit an increase in intensity, they are blue-shifted in comparison to their respective solution counterparts. This phenomenon could be attributed to the formation of a larger proportion of disordered aggregates during solvent evaporation.[23]

Detailed analysis of the UV-vis absorption spectra provides further insights relating to polymer chain conjugation length (intramolecular ordering).[4,24] Examination of the P3HT absorption spectrum reveals bands associated with two phases, a crystalline region due to ordered chains and an amorphous

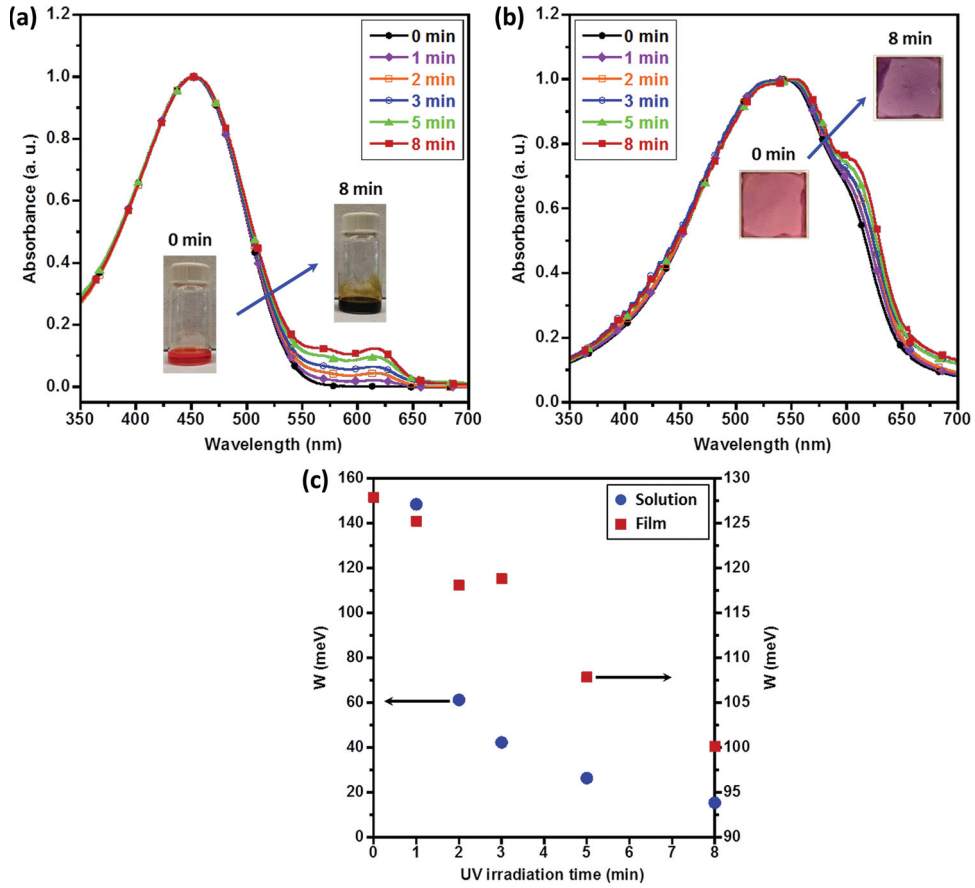

Figure 3. Normalized UV-visible absorption spectra of a) P3HT/$CHCl_3$ solutions as a function of UV irradiation time and b) corresponding P3HT films obtained by spin-coating. c) The evolution of exciton bandwidth *W* of ordered aggregates in the solutions and films as a function of UV irradiation time. The inset images in Figure 3a show the color change of P3HT/$CHCl_3$ solution from bright orange to dark brown by UV irradiation for 8 min while the inset images in Figure 3b represent the corresponding films which exhibit different colors, pale red and dark purple, respectively.

region due to disordered chains.[24] According to Spano's model, the crystalline regions are assumed to be composed of weakly interacting H-aggregates in which interchain coupling leads to vibronic bands in the absorption spectrum.[24] Further, the vibronic bands can be related to the free exciton bandwidth (*W*) which correlates with the conjugation length (intrachain ordering) of an individual polymer chain.[4,23,24] A decrease in *W* indicates an increase in both average conjugation length and chain order.[4,24] The *W* values are calculated using Equation 1 and the intensities of the (0–0) and (0–1) transitions obtained from fits to the experimental spectra (see Supporting Information Figure S7,S8).

$$\frac{I_{0-0}}{I_{0-1}} \approx \left(\frac{1-0.24W/E_p}{1+0.073W/E_p} \right)^2 \quad (1)$$

I_{0-0} and I_{0-1} are the intensities of the (0–0) and (0–1) transitions, respectively and E_P is the the vibrational energy of the symmetric vinyl stretch (taken as 0.18 eV).[24] Polymer intrachain ordering in solution is found to be enhanced by UV irradiation based on observed decreasing free exciton bandwidth with increased UV irradiation time (from 148.42 to 15.37 meV) as shown in Figure 3c. *W* of the pristine polymer solution could not be calculated because no aggregates were detected in the solution. UV irradiation of the polymer solutions evidently impacts intra- and intermolecular ordering of resultant polymer films; as the irradiation time increases, the intensity of the low energy features increases (Figure 3b), while *W* decreases from 127.90 to 100.13 meV in the corresponding polymer thin-films (Figure 3c). *W* calculated from the solution spectra has lower values than *W* of the corresponding films; the solution based nanoaggregates formed upon UV irradiation are thus suggested to contain a higher degree of well-ordered polymer chains while the aggregates in the corresponding films present more disordered polymer chains formed during solvent evaporation together with well-ordered polymer chains formed by UV irradiation of the precursor solutions.

The enhanced intra- and intermolecular interactions of P3HT chains are expected to lead to higher thin-film crystallinity.[3c,13a] **Figure 4**a shows X-ray diffractograms obtained from grazing incidence (GIXD) measurements of P3HT films spin-coated from P3HT/$CHCl_3$ solutions irradiated by UV for a series of different times. Increase in UV irradiation time of the precursor solutions effects a gradual increase in intensity of the (100) peak associated with polymer chain lamellar packing along the crystallographic direction perpendicular to the backbone. This increase could result from either an increase in the size of individual crystallites, the number of crystallites, or both.[3c,13a]

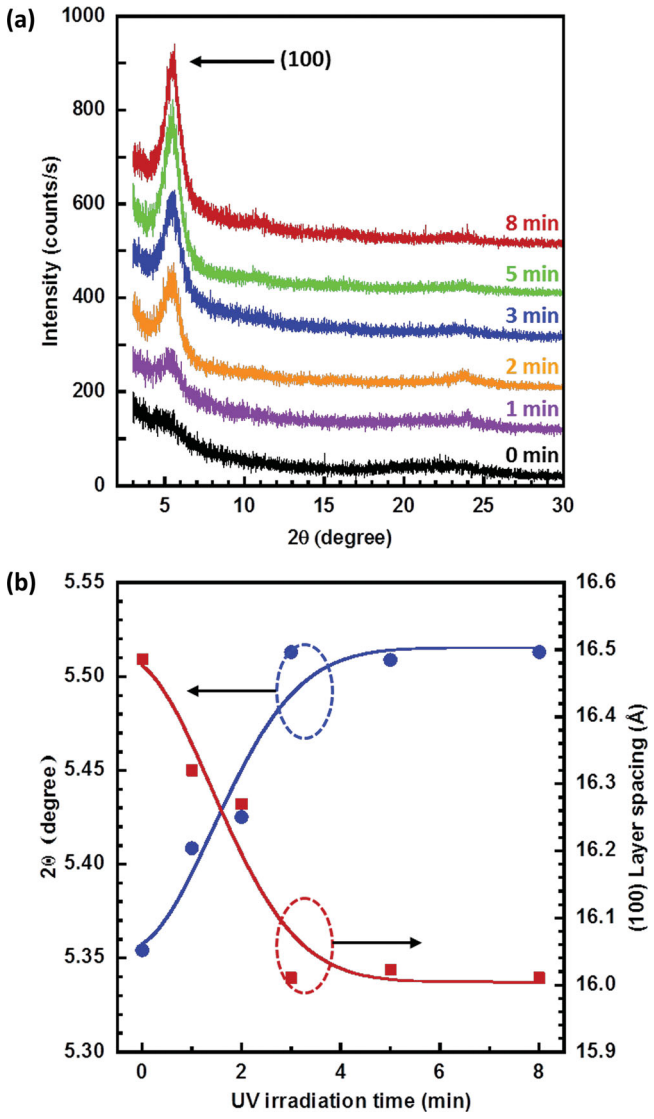

Figure 4. a) Grazing incidence X-ray diffraction profiles of P3HT films obtained from the UV irradiated solutions. b) 2θ angle (left axis) of the (100) peak and corresponding layer spacing (right axis) as a function of precursor solution UV irradiation time.

The micro-structural change is further characterized by a (100) peak shift to higher angle, from 5.35 to 5.51° after 8 min of UV irradiation, indicative of a decrease in d-spacing in the direction along the side chains from 16.49 to 16.01 Å (Figure 4b) and suggestive of either increased interdigitation between P3HT alkyl side chains or a change in side chain tilt.[3c,13a]

The morphological change of the resultant films is also observed through polarized optical microscopy (POM) as shown in **Figure 5**. With increased UV irradiation time, images of the resultant thin-films as observed through crossed polarizers appear to brighten. While the film cast from a pristine solution appears dark and therefore isotropic (amorphous), the films cast from solutions exposed to UV for longer durations exhibit increasingly bright birefringent textures. The observed birefringence is another indicator for either enhanced conjugated polymer molecular ordering or crystallinity.[25]

Atomic force microscopy (AFM) images of P3HT films obtained from pristine and UV irradiated P3HT solutions are shown in **Figure 6**, demonstrating the clear evolution of anisotropic growth of P3HT aggregates from an initial featureless and amorphous-like structure. In solution, UV irradiation induced polymer backbone planarization would lead to nanofibrillar structured aggregates via favorable π–π stacking of the polymer chains. For instance, UV irradiation of the solutions for a short time (≈1 min) leads to the formation of distinct nanofibrils that are ≈30 nm in width and 300–600 nm in length. Increased irradiation time affords not only an increased number of nanofibers, but their length also increases substantially (>1 μm). The surface roughness of resultant films also changed upon UV exposure. The pristine films show a relatively low root-mean square (RMS), ≈0.63 nm, while the RMS of films obtained from UV irradiated solutions gradually increases up to ≈1.97 nm with increased UV irradiation time. The increased roughness is ascribed to the increase size and quantity of nanofibrillar structures within the thin-films.

The AFM, XRD, and POM results are in good agreement, suggesting that the increase in the degree of polymer thin-film crystallinity is a direct consequence of the increased number and size of microcrystallite-like P3HT nanofibers formed in the precursor solutions during UV irradiation, which are then distributed throughout the solidified films via the spin-coating process. In contrast, the crystalline nanofibers formed within P3HT films obtained from ultrasonicated solutions are shorter (<300 nm vs >1 μm) (Supporting Information, Figure S9a,b), generating relatively more grain boundaries resistive to efficient charge carrier transport.[3c] Thus, the resultant films prepared from ultrasonicated solutions exhibit lower macroscopic mobilities compared to those obtained from UV treatment, even though the former exhibit an enhanced degree of molecular ordering and presumably higher crystallinity (see Supporting Information Figure S9c,d). These results underscore the significance of grain boundaries, in addition to ordering and/or crystallinity in achieving efficient charge transport within π-conjugated polymer films. To maximize semiconducting polymer thin-film charge transport characteristics, the number of grain boundaries within the polymer films should be reduced while the molecular ordering should be enhanced.

UV irradiation of P3HT solutions prepared in non-chlorinated solvents was also found to facilitate molecular ordering. For instance, irradiation of P3HT/toluene effects dramatic enhancement of charge carrier transport within corresponding films as shown in **Figure 7**. In toluene solution, the P3HT absorption spectrum exhibits low energy features at ≈570 and 620 nm, characteristic of well-ordered UV irradiation induced aggregate formation (Figure 7a). The solution based nanoaggregates survive a spin-coating process, and provide for enhanced molecular order in the solid thin-films (Figure 7b). While thin-films derived from P3HT/chloroform appear amorphous-like (Figure 6a), those obtained from P3HT/toluene solution are composed of many small nanofibrillar structures (Figure 7c); the lower evaporation rate of toluene vs. chloroform may facilitate polymer chain interactions, alignment and stacking into fibrillar structures during the coating process. In contrast to the pristine sample, the P3HT film obtained from a UV irradiated (8 min) P3HT/toluene solution exhibits noticeably wider

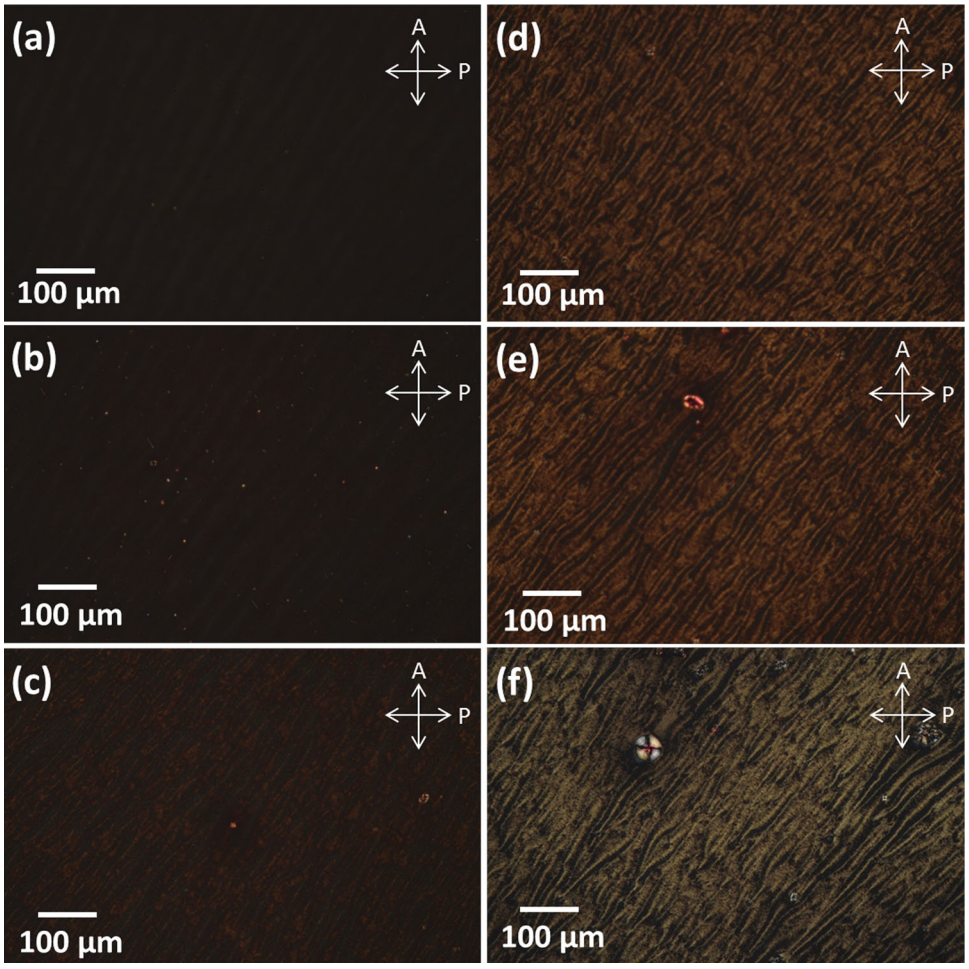

Figure 5. Polarized optical microscopic images of P3HT films spin-coated on glass from P3HT/$CHCl_3$ solutions UV irradiated for a) 0, b) 1, c) 2, d) 3, e) 5, and f) 8 min. All images were taken with crossed polarizers.

and longer fibrils, in addition to the small fibrillar aggregates (Figure 7d). As with the chloroform solution, UV irradiation of P3HT/toluene effects an increase in P3HT charge carrier mobility. As shown in Figure 7e, mobility increased by a factor of approximately 9, from $0.42 \pm 0.02 \times 10^{-2}$ cm^2 V^{-1} s^{-1} to $3.7 \pm 0.42 \times 10^{-2}$ cm^2 V^{-1} s^{-1}.

3. Conclusions

In conclusion, the anisotropic supramolecular assembly of P3HT chains in solution can be achieved simply via short (<8 min), low-intensity UV irradiation. Polymer degradation was not discernible, and exposure to a low UV dose led to enhanced molecular ordering in solution with resultant dramatic enhancement of corresponding thin-film charge transport characteristics. UV induced enhanced polymer chain intramolecular ordering in solution, and thereby effected formation of anisotropic supramolecular assemblies via favorable π-π stacking (intermolecular interaction) of the polymer chains. The nanofibrillar aggregates formed in solution survived the film deposition process and in turn, evidently enhanced the supramolecular ordering and charge transport characteristics of resultant polymer films. The crystalline-like nanofibrillar aggregates appeared relatively long (>1 µm) compared to those obtained in films prepared via ultrasonic irradiation, contributing to dramatic improvement of charge carrier mobilities, presumed to arise from a reduction in the number of grain boundaries. Low-dose UV irradiation presents a strategy for enhancing anisotropic molecular ordering of π-conjugated polymers in precursor solution thereby eliminating the need for process steps such as dielectric surface modification or thermal and/or solvent vapor annealing of the polymer thin-films. The approach may prove attractive in the pursuit of robust, low-cost, large-area electronic device fabrication methodologies.

4. Experimental Section

Materials: P3HT and P3BT were purchased from Rieke Metals Inc., and used without further purification. The molecular weight of P3HT (M_n of 19.7 kDa and M_w of 43.7 kDa) and P3BT (M_n of 25.8 kDa and M_w of 55.5 kDa) used for the study was obtained through gel permeation

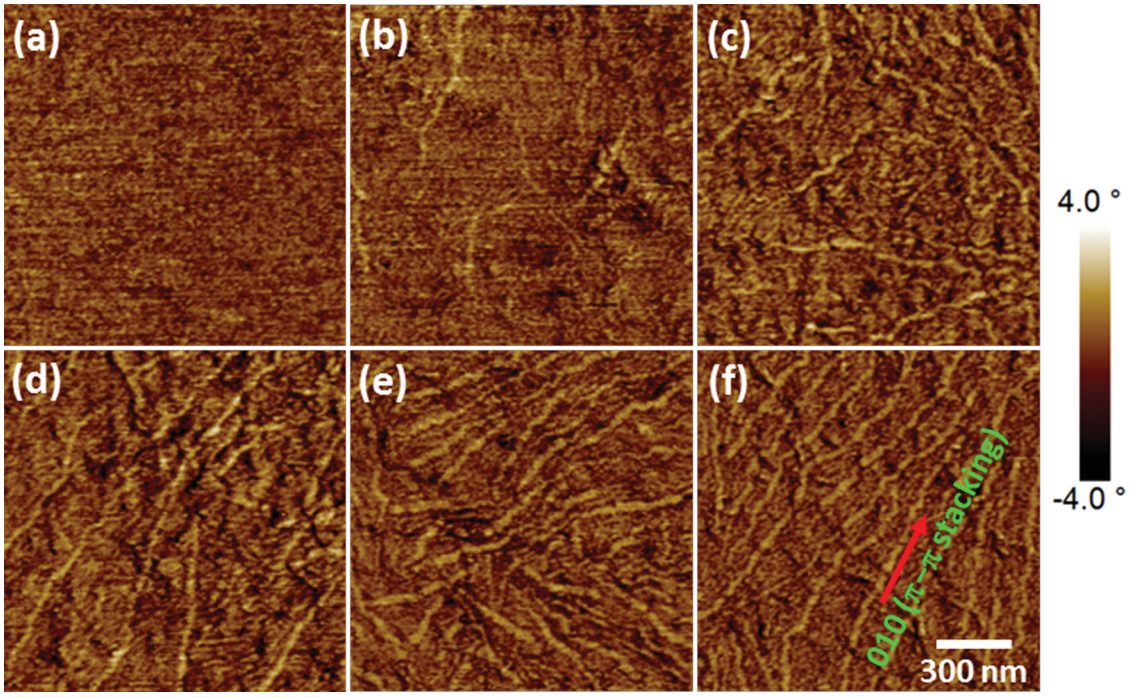

Figure 6. Tapping mode AFM phase images of P3HT films obtained by spin-coating from P3HT/$CHCl_3$ solutions UV irradiated for a) 0, b) 1, c) 2, d) 3, e) 5, and f) 8 min.

chromatography (GPC) using trichlorobenzene as the eluent and polystyrene as standard. The head to tail regioregularity (RR) was estimated to be approximately 96% for P3HT and 87% for P3BT from the 1H-NMR spectra obtained from deuterated chloroform solution at 293 K using a Bruker DSX 300. Chloroform used in this study was anhydrous grade, purchased from Sigma Aldrich, and used without further purification.

Anisotropic Growth of P3HT Aggregates in Solution: 10 mg of P3HT was introduced into 2 mL of chloroform in a 20 mL borosilicate glass vial fitted with a magnetic stir bar in air. Alternatively, 6 mg of P3HT was introduced into 2 mL of toluene, owing to the relatively lower solubility of P3HT in toluene. Subsequently, the vial was sealed with a cap and the solution was stirred for at least 30 min at ≈55 °C to ensure complete polymer dissolution. The as-prepared solution was cooled to ambient temperature prior to UV irradiation. The vial containing the solution was placed on a hand-held UV lamp (Entela UVGL-15, 5 mW cm^{-2}, 254 nm) which had been placed on a magnetic stirrer (Corning Inc.). Then, the solution was gently stirred and simultaneously irradiated for times ranging from 0 to 8 min. The irradiation was performed through the bottom wall of the borosilicate glass vial which transmits more than 90% of the incident UV 254 nm light. P3HT nanofibrillar aggregates began to appear in the solution and further, increased in both quantity and size with increased irradiation time. The ultrasonic irradiation of P3HT solutions was performed by following the published procedure.[13a]

Organic Field-Effect Transistor (OFET) Fabrication and Characterization: The OFET devices used for electrical characterization consisted of two contact devices where P3HT films were deposited via spin-coating the relevant polymer solution onto a 300 nm thick SiO_2 gate dielectric. The highly doped silicon substrate served as the gate electrode while Au/Cr was used for the source and drain contacts. The source and drain contacts were fabricated using a standard photolithography based lift-off process, followed by E-beam evaporation (Denton Explorer) of 50 nm Au contacts with 3 nm of Cr as the adhesion layer. Before spin-coating P3HT solutions, all devices were cleaned for 15 min in a UV-ozone cleaner (Novascan PSD-UV) to completely remove any residual photoresist and other organic contaminants. OFET devices were prepared by spin-coating (WS-650MZ-23NPP, Laurell) the solutions onto precleaned substrates at a spin speed of 1500 rpm for 60 s in air, and tested in nitrogen ambient using an Agilent 4155C semiconductor parameter analyzer. The polymer films spin-coated from the P3HT solutions treated by UV irradiation for times in the range of 0 to 8 min were found to have similar thickness, in the range of 26–30 nm, as determined by spectroscopic ellipsometry (M-2000, JA Woollam). The devices were stored in a vacuum oven (1 Torr) overnight at room temperature to remove residual solvent. The field-effect hole mobility was calculated in the saturation regime of transistor operation (V_{DS} = –80 V) by plotting the drain current (I_{DS}) versus gate voltage (V_{GS}) and fitting the data to the following equation:[26]

$$I_{DS} = \frac{WC_{OX}}{2L}\mu(V_{GS} - V_T)^2 \quad (2)$$

where W (2000 μm) and L (50 μm) are the transistor channel width and length, respectively, V_T is the threshold voltage, and C_{OX} is the capacitance per unit area of the silicon dioxide gate dielectric (1.15 × 10^{-8} F cm^{-2}).

UV-Vis Spectroscopy: The solution and solid state UV-vis spectra were recorded using an Agilent 8510 UV-vis spectrometer. Films for solid state studies were prepared by spin-coating the requisite solution onto precleaned glass slides following the same procedures used to prepare OFET devices.

Grazing Incidence X-Ray Diffraction (GIXD): Out-of-plane grazing incidence X-ray diffraction data were obtained using a Panalytical X'Pert Pro system equipped with a Cu X-ray source operating at 45 kV and 40 mA. The grazing incidence angle was fixed at 0.2° and the detector was scanned from 3° to 30°.

Atomic Force Microscopy (AFM): The AFM measurements were performed on films spin-coated onto bottom contact OFET devices using an ICON dimension scanning probe microscope (Bruker) operating in tapping mode with a silicon tip (RTESP, Bruker).

Polarized Optical Microscopy (POM): The POM images were obtained with a Leica DMRX optical microscope equipped with a polarizer and a Nikon D300 digital SLR camera.

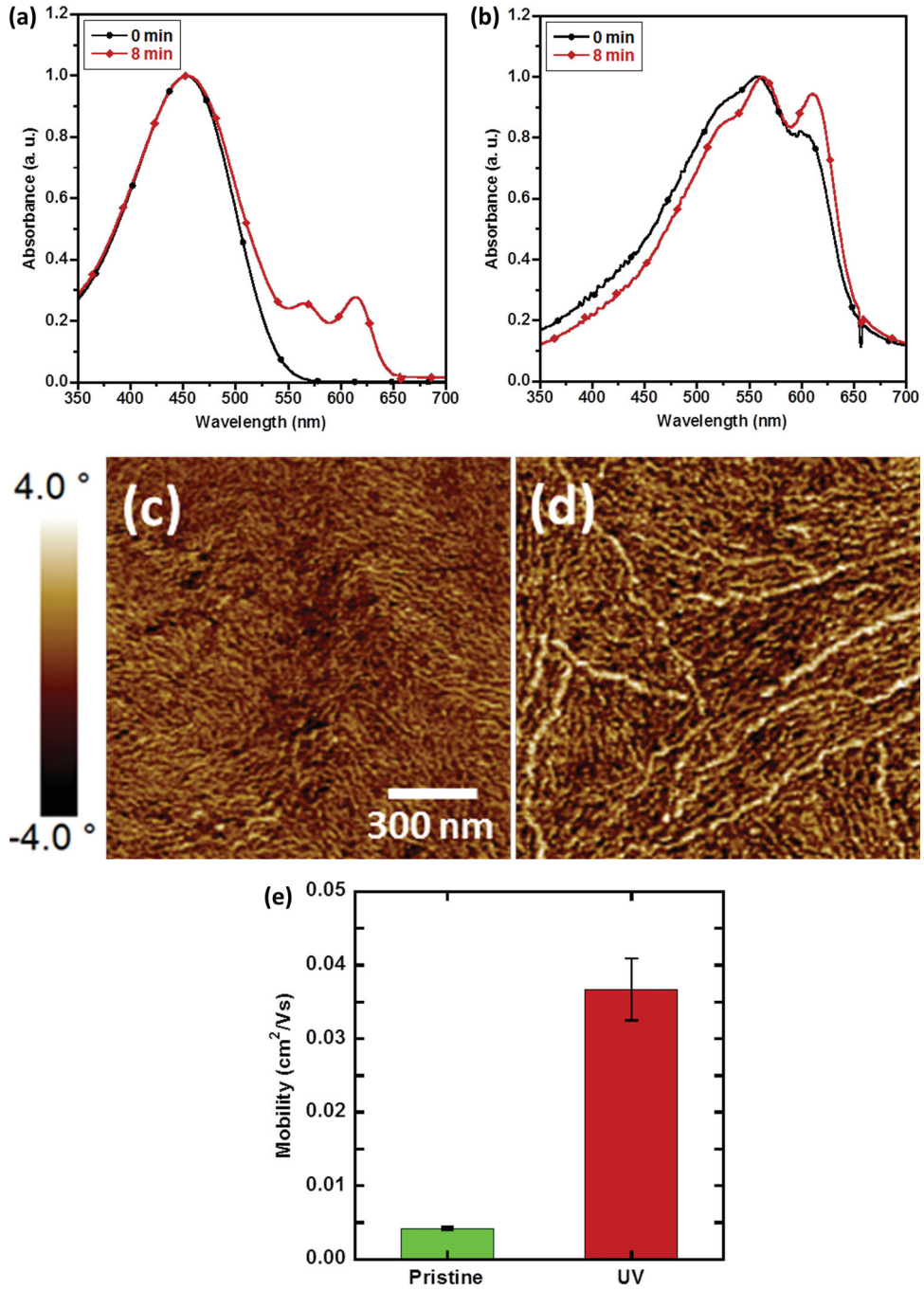

Figure 7. Normalized UV-visible absorption spectra of a) P3HT/Toluene solutions before and after 8 min UV irradiation. b) corresponding P3HT films obtained by spin-coating. Tapping mode AFM phase images of P3HT films obtained by spin-coating from P3HT/Toluene solutions c) before and d) after 8 min UV irradiation. e) Field-effect mobilities of corresponding films.

Supporting Information

Supporting Information is available from the Wiley Online Library or from the author.

Acknowledgements

The financial support of the Georgia Institute of Technology and the Air Force Office of Scientific Research (FA9550–12–1–0248) is gratefully acknowledged. The authors would also like to thank Tae-Seop Choi at the Georgia Institute of Technology for his help with XPS experiments and Ben Cherniawski and Prof. Alejandro L. Briseno at the University of Massachusetts Amherst for their help with GPC experiments presented in Supporting Information.

Received: February 14, 2014
Published online: April 14, 2014

[1] a) J. H. Li, Z. H. Sun, F. Yan, *Adv. Mater.* **2012**, *24*, 88; b) H. Yan, Z. H. Chen, Y. Zheng, C. Newman, J. R. Quinn, F. Dotz, M. Kastler, A. Facchetti, *Nature* **2009**, *457*, 679; c) S. R. Forrest, *Nature* **2004**, *428*, 911; d) G. Li, R. Zhu, Y. Yang, *Nat. Photonics* **2012**, *6*, 153.
[2] a) M. O'Neill, S. M. Kelly, *Adv. Mater.* **2011**, *23*, 566; b) B.-G. Kim, E. J. Jeong, J. W. Chung, S. Seo, B. Koo, J. Kim, *Nat. Mater.* **2013**.
[3] a) V. Coropceanu, J. Cornil, D. A. da Silva, Y. Olivier, R. Silbey, J. L. Bredas, *Chem. Rev.* **2007**, *107*, 926; b) S. Goffri, C. Muller, N. Stingelin-Stutzmann, D. W. Breiby, C. P. Radano, J. W. Andreasen, R. Thompson, R. A. J. Janssen, M. M. Nielsen, P. Smith, H. Sirringhaus, *Nat. Mater.* **2006**, *5*, 950; c) M. Chang, D. Choi, B. Fu, E. Reichmanis, *ACS Nano* **2013**.
[4] A. R. Aiyar, J. I. Hong, E. Reichmanis, *Chem. Mater.* **2012**, *24*, 2845.
[5] H. Sirringhaus, P. J. Brown, R. H. Friend, M. M. Nielsen, K. Bechgaard, B. M. W. Langeveld-Voss, A. J. H. Spiering, R. A. J. Janssen, E. W. Meijer, P. Herwig, D. M. de Leeuw, *Nature* **1999**, *401*, 685.
[6] A. R. Aiyar, J. I. Hong, J. Izumi, D. Choi, N. Kleinhenz, E. Reichmanis, *ACS Appl. Mater. Interfaces* **2013**, *5*, 2368.
[7] J. F. Chang, B. Q. Sun, D. W. Breiby, M. M. Nielsen, T. I. Solling, M. Giles, I. McCulloch, H. Sirringhaus, *Chem. Mater.* **2004**, *16*, 4772.
[8] D. H. Kim, Y. Jang, Y. D. Park, K. Cho, *Langmuir* **2005**, *21*, 3203.
[9] a) Y. Fu, C. Lin, F. Y. Tsai, *Org. Electron.* **2009**, *10*, 883; b) S. Cho, K. Lee, J. Yuen, G. M. Wang, D. Moses, A. J. Heeger, M. Surin, R. Lazzaroni, *J. Appl. Phys.* **2006**, *100*, 114503.
[10] a) R. J. Kline, M. D. McGehee, E. N. Kadnikova, J. S. Liu, J. M. J. Frechet, *Adv. Mater.* **2003**, *15*, 1519; b) R. Zhang, B. Li, M. C. Iovu, M. Jeffries-EL, G. Sauve, J. Cooper, S. J. Jia, S. Tristram-Nagle, D. M. Smilgies, D. N. Lambeth, R. D. McCullough, T. Kowalewski, *J. Am. Chem. Soc.* **2006**, *128*, 3480.
[11] a) N. Kiriy, E. Jahne, H. J. Adler, M. Schneider, A. Kiriy, G. Gorodyska, S. Minko, D. Jehnichen, P. Simon, A. A. Fokin, M. Stamm, *Nano Lett.* **2003**, *3*, 707; b) L. G. Li, D. L. Jacobs, Y. K. Che, H. L. Huang, B. R. Bunes, X. M. Yang, L. Zang, *Org. Electron.* **2013**, *14*, 1383.
[12] a) J. S. Kim, J. H. Lee, J. H. Park, C. Shim, M. Sim, K. Cho, *Adv. Funct. Mater.* **2011**, *21*, 480; b) J. Y. Oh, M. Shin, T. I. Lee, W. S. Jang, Y. Min, J. M. Myoung, H. K. Baik, U. Jeong, *Macromolecules* **2012**, *45*, 7504.
[13] a) A. R. Aiyar, J. I. Hong, R. Nambiar, D. M. Collard, E. Reichmanis, *Adv. Funct. Mater.* **2011**, *21*, 2652; b) B. G. Kim, M. S. Kim, J. Kim, *ACS Nano* **2010**, *4*, 2160.
[14] L. H. Jimison, M. F. Toney, I. McCulloch, M. Heeney, A. Salleo, *Adv. Mater.* **2009**, *21*, 1568.
[15] a) L. L. Chua, J. Zaumseil, J. F. Chang, E. C. W. Ou, P. K. H. Ho, H. Sirringhaus, R. H. Friend, *Nature* **2005**, *434*, 194; b) P. T. Wu, H. Xin, F. S. Kim, G. Q. Ren, S. A. Jenekhe, *Macromolecules* **2009**, *42*, 8817.
[16] a) J. Ruhe, N. F. Colaneri, D. D. C. Bradley, R. H. Friend, G. Wegner, *J. Phys.: Condens. Matter* **1990**, *2*, 5465; b) Y. H. Kim, D. Spiegel, S. Hotta, A. J. Heeger, *Phys. Rev. B* **1988**, *38*, 5490.
[17] a) Y. J. Cheng, S. H. Yang, C. S. Hsu, *Chem. Rev.* **2009**, *109*, 5868; b) B. Xu, S. Holdcroft, *Macromolecules* **1993**, *26*, 4457; c) A. G. MacDiarmid, *Angew. Chem. Int. Ed.* **2001**, *40*, 2581.
[18] J. L. Bredas, R. R. Chance, R. Silbey, *Phys. Rev. B* **1982**, *26*, 5843.
[19] J. F. Mike, K. Nalwa, A. J. Makowski, D. Putnam, A. L. Tomlinson, S. Chaudhary, M. Jeffries-EL, *Phys. Chem. Chem. Phys.* **2011**, *13*, 1338.
[20] H. J. Son, B. Carsten, I. H. Jung, L. P. Yu, *Energy Environ. Sci.* **2012**, *5*, 8158.
[21] J. M. Zhuo, L. H. Zhao, R. Q. Png, L. Y. Wong, P. J. Chia, J. C. Tang, S. Sivaramakrishnan, M. Zhou, E. C. W. Ou, S. J. Chua, W. S. Sim, L. L. Chua, P. K. H. Ho, *Adv. Mater.* **2009**, *21*, 4747.
[22] H. Hintz, H. J. Egelhaaf, L. Luer, J. Hauch, H. Peisert, T. Chasse, *Chem. Mater.* **2011**, *23*, 145.
[23] G. Nagarjuna, M. Baghgar, J. A. Labastide, D. D. Algaier, M. D. Barnes, D. Venkataraman, *ACS Nano* **2012**, *6*, 10750.
[24] J. Clark, J. F. Chang, F. C. Spano, R. H. Friend, C. Silva, *Appl. Phys. Lett.* **2009**, *94*, 163306.
[25] a) L. Kinder, J. Kanicki, P. Petroff, *Synth. Met.* **2004**, *146*, 181; b) E. J. W. Crossland, K. Rahimi, G. Reiter, U. Steiner, S. Ludwigs, *Adv. Funct. Mater.* **2011**, *21*, 518.
[26] G. Horowitz, R. Hajlaoui, H. Bouchriha, R. Bourguiga, M. Hajlaoui, *Adv. Mater.* **1998**, *10*, 923.